

## Interaction between proteins of the PPAR $\gamma$ and NF $\kappa$ B immune response pathways and rotavirus non-structural proteins

Dory Gómez, Carlos A. Guerrero\*

Department of Physiological Sciences, Faculty of Medicine, Universidad Nacional de Colombia, Bogota, Capital District, Colombia

Received May 25, 2021; revised August 16, 2021; accepted January 18, 2022

**Summary.** – Cells infected with MA104 rotavirus and/or transfected with plasmids expressing NSP proteins, were analyzed for expression of cellular proteins related to NF $\kappa$ B and PPAR $\gamma$  pathways and evaluated through the ELISA, luminescence, flow cytometry and Western blot techniques. The association between cellular and viral (NSPs) proteins was examined by ELISA, epifluorescence and confocal microscopy techniques. It was observed that NSP1 protein interacts with RXR, NSP1, and NSP3 with PPAR $\gamma$ , NSP2 with p-IKK $\alpha/\beta$  and NSP5 with NF $\kappa$ B proteins. We have found that phosphorylated PPAR $\gamma$  is localized in cytoplasm and transcriptional activity of PPRE is diminished. These results lead to the conclusion, that RRV activates the proinflammatory pathway, increasing the expression of NF $\kappa$ B and possibly by PPAR $\gamma$  phosphorylation, its translocation to the nucleus is impeded, thus inactivating the proinflammatory pathway.

**Keywords:** rotavirus; PPAR $\gamma$ ; NF $\kappa$ B; NSPs; RRV

### Introduction

Rotaviruses belong to the *Reoviridae* family containing non-enveloped icosahedral viruses. They measure approximately 70 nm in diameter; its genome comprises of a double-stranded RNA, which encodes six structural proteins called VP1-VP4, VP6, VP7 and six nonstructural proteins called NSP1 to NSP6 (Crawford *et al.*, 2017; Pesavento *et al.*, 2006; Estes and Cohen, 1989). The virus enters the host cell by interaction with cellular proteins found in the cellular membrane such as sialic acid (Isa *et al.*, 2006), heat shock protein (Zárate *et al.*, 2003; Wang *et al.*, 2020; Rico *et al.*, 2020; Guerrero and Moreno, 2012), dynamin protein (Gutiérrez *et al.*, 2010), integrins (Guerrero *et al.*,

2000; Londrigan *et al.*, 2000; Zárate *et al.*, 2000), and protein disulfide-isomerase (Moreno *et al.*, 2016; Rivera *et al.*, 2020). Depending on strain, the virus enters the cells using different endocytosis pathways (Arias *et al.*, 2015). Replication and assembly of the rotavirus genome takes place in cytoplasmic inclusions called viroplasm (VP). During the viral infection, rotavirus nonstructural proteins participate in different intracellular processes. They are involved in antagonizing the antiviral host response and subverting important cellular processes to enable successful virus replication (Trujillo *et al.*, 2011; Sen *et al.*, 2020). Furthermore, it is known that oxidative stress is part of the cellular process during virus infection (Guerrero and Acosta, 2016) and can be a mechanism by which viruses damage cells (Echeverri and Mockus, 2010; Fuchs and Flügge, 2004). The interaction between oxidative stress and viral infection (Schwarz, 1996; Ivanov *et al.*, 2017; Camini *et al.*, 2017) and the mechanisms that lead to cell death (Guerrero and Acosta, 2016) have been documented. During the first hours post-infection, the nonstructural protein 1 (NSP1) antagonizes the immune host response (Sen *et al.*, 2009; Barro and Patton, 2005; Feng *et al.*, 2009).

\*Corresponding author. E-mail: caguerrero@unal.edu.co; phone: +3165000-15052, 15053 or 15047.

**Abbreviations:** CUR = curcumin; h.p.i. = hours post-infection; h.p.t. = hours post-transfection; NF $\kappa$ B = nuclear factor kappa B; NSPs = nonstructural proteins; PPAR $\gamma$  = peroxisome proliferator-activated receptor gamma; ROS = reactive oxygen species; TZD = thiazolidinedione; PGZ = pioglitazone; VP = viroplasm

NSP1 inhibits NF $\kappa$ B activation by degradation of  $\beta$ -TrCP (Graff *et al.*, 2009). The nonstructural protein 3 (NSP3) binds to cellular translation machinery and permits mRNA viral cellular translation (Firth and Brierley, 2012). NSP3 is involved in cellular mRNA inhibition by binding to eIF4G (Piron *et al.*, 1998; Deo *et al.*, 2002). During rotavirus infection, the nonstructural protein 4 (NSP4) is known to interrupt calcium ( $\text{Ca}^{2+}$ ) cellular homeostasis through translocation to the endoplasmic reticulum and the mitochondria (Bhowmick *et al.*, 2012). NSP4 exerts its pro-apoptotic effect by interacting with mitochondrial proteins, although apoptosis activation by NSP4 is inhibited by the activation of cell survival pathways (PI3K /Akt) by NSP1 during the first hours of infection (Bhowmick *et al.*, 2012). However, the relationship between proteins of the peroxisome proliferator-activated receptor gamma (PPAR $\gamma$ ) and nuclear factor kappa B (NF $\kappa$ B) immune response pathway and rotaviral nonstructural proteins is not fully characterized.

Researchers have reported that PPAR $\gamma$  activation by thiazolidinedione (TZD) (Hsieh *et al.*, 2010; Potula *et al.*, 2008; Jarrar and Baranova, 2007) interferes with the NF $\kappa$ B signaling cascade, which leads to a reduction in the transcription of some pro-inflammatory genes depending on NF $\kappa$ B. The negative interference mediates part of the PPAR anti-inflammatory regulation between the PPAR and other nuclear factors like NF $\kappa$ B, AP-1, and C/EBP, regulating innate and adaptative immunity (Genolet *et al.*, 2004). Additionally, the ligands of PPAR $\gamma$  inhibit the expression of inflammatory genes like interleukin 1 $\beta$  and the tumor necrosis factor- $\alpha$  (Clark, 2002). Treatment with a PPAR $\gamma$  agonist increases PPAR $\gamma$  levels (Yeligar *et al.*, 2017). The above supports the potential role of PPAR $\gamma$  agonists for viral infection treatment. Additionally, rotavirus infection induces an inflammatory response in the host cell, accompanied by an increase in expression or activation of some molecules, including reactive oxygen species (ROS), NF $\kappa$ B, and COX-2 (Gómez *et al.*, 2016). Stimulation with PPAR $\gamma$  agonists pioglitazone, thiazolidinedione, rosiglitazone, docosahexaenoic acid, alpha lipoic acid, all-trans retinoic acid, and treatment with N-acetylcysteine interfere with viral infections, including rotavirus infection (Gómez *et al.*, 2016; Guerrero *et al.*, 2012, 2013). The accumulation of the studied cellular proteins and ROS, induced by rotavirus infection, was reduced with pioglitazone (PGZ) treatment, causing a concomitant reduction in the infectious virion's performance. However, the relation between NF $\kappa$ B and PPAR $\gamma$  cellular pathways with rotavirus infections is not yet clear, as they affect opposite pathways (Gómez *et al.*, 2016; Villapol, 2018; Martin, 2010; Kapadia *et al.*, 2008; Liu *et al.*, 2007; Lawrence, 2009). Similarly, it has not been determined yet if rotavirus proteins are implied directly in the increase in expression of cel-

lular proteins, or the increase is due to the cell's response to the viral infection.

Therefore, this research intended to determine possible interactions between RRV rotavirus nonstructural proteins (NSP1, NSP2, NSP3, NSP4, NSP5, and NSP6) with proteins from the PPAR $\gamma$ -NF $\kappa$ B pathway in MA104 cells. For this purpose, the expression of cellular proteins related to the NF $\kappa$ B and PPAR $\gamma$  pathway was evaluated in MA104 cells infected and/or transfected with rotavirus NSPs proteins. We found that NSP1 interacts with RXR, NSP1 and NSP3 with PPAR $\gamma$ , NSP2 with p-IKK $\alpha$ / $\beta$ , and NSP5 with NF $\kappa$ B 12 hours post-infection (h.p.i). Additionally, we observed that phosphorylated PPAR $\gamma$  is found in the cytoplasm, and the transcriptional activity of PPRE is diminished. Finally, we conclude that RRV activates the inflammatory pathway, increasing the expression of NF $\kappa$ B, and possibly by phosphorylation of PPAR $\gamma$ , its translocation to the nucleus is impeded, leading to inactivation of the anti-inflammatory pathway.

## Materials and Methods

**Bacterial strains and plasmids.** The *E. coli* bacterial strains XL1-BLUE, DH5 $\alpha$  (Taylor *et al.*, 1993), BL21 (DE3) were used for the plasmid amplification and protein expression. Bacteria were grown in Luria-Bertani (LB) broth and agar. Used plasmids are presented in Supplementary Table S1. To express rotavirus NSPs in the eukaryotes, the relevant DNA segments were cut with restriction enzymes from the prokaryotic expression plasmids: pGEM 3ZNSP1 (SmaI and HindIII), pET-28a NSP2 (HindIII and BamHI), pET-28a NSP3 (XhoI and BstEII), pET-28a NSP4 (HindIII and BamHI) and pET-28a NSP5 (HindIII and BamHI). The procedure of digestion, inactivation, and ligation was carried out according to the protocols described for each restriction enzyme by manufacturers (BioLabs, USA; Thermo Fisher, USA).

**Rotavirus strains, antibodies, and reagents.** Dr. Carlos Arias from Universidad Nacional Autónoma de México kindly provided the RRV (Rhesus rotavirus). The MOI of 0.8 was used (Guerrero *et al.*, 2012). The MTT assay was used to determine the cell viability at different time-points post-transfection. The plates were read at 590 nm on a Stat Fax 303/Plus reader (Awareness Technology, Inc., USA). Antibodies and reagents are presented in Supplementary Table S2.

**Transformation and plasmid isolation.** Bacteria XL1-BLUE, BL21 or DH5 $\alpha$  with an optical density of 0.5 (approximately  $600 \times 10^6$  bacteria/ml) were mixed with 10 ng of plasmid DNA and processed as described previously (Moreno *et al.*, 2013). The *E. coli* DH5 $\alpha$  bacteria, in LB media, were transformed with different plasmids independently, taking into account the characteristics of each plasmid. Extraction and purification of plasmids was performed by the Column-pure plasmid miniprep kit (Applied Biological Materials Inc, Canada). Plasmids were

quantified by NanoDrop<sup>TM</sup>, ND-1000 (Thermo Fisher, USA). The plasmids were treated with specific restriction enzymes and were analyzed in agarose gel. The isolated plasmids were kept at -20°C until use.

*Expression of recombinant proteins in prokaryotic cells and their isolation.* Ten  $\mu$ l of each of the transformed bacteria with each plasmid of interest, with an optical density of 0.5 were incubated in 10 ml of LB medium over night at 37°C, in the presence of ampicillin or kanamycin antibiotics (100  $\mu$ g/ml, final concentration). The expression of the recombinant proteins was carried out as previously described (Moreno *et al.*, 2016).

*SDS-PAGE and electroelution of proteins.* The bacterial lysate was separated by SDS-PAGE electrophoresis in 10% or 12% gels in denaturing/reducing conditions. The 26,61 mg/ml of proteins in a 200  $\mu$ l volume in duplicates were separated. Half of the gel was transferred, in semidry conditions, to a PVDF membrane. The membrane was blocked with 5% skimmed milk and detected by a hyperimmune anti-rabbit serum against NSP4, NSP5, or anti-guinea pig or mouse anti-PPAR $\gamma$  antibody. IgG-HRP secondary antibodies were used (0.4  $\mu$ g/ml Santa Cruz, USA). The proteins were visualized with aminoethyl carbazole 0.64 mg/ml (AEC, Sigma-Aldrich, USA), acetate buffer pH 5 and 0.36% hydrogen peroxide, for 45 min. Once the bands were identified by Western blot, the bands of interest were cut out of the other half of the gel and were electroeluted. The electroelution was carried out for 3 h, at constant 10 mA per tube, in running buffer (192 mM glycine, 25 mM Tris, SDS 0.1% pH 8.3) in a camera model 422 (Bio Rad<sup>®</sup>, USA). The electroeluted proteins were precipitated with acetone (1:3 v:v, protein: acetone) overnight at -80°C and were centrifuged at 11,200  $\times$  g for 30 min at 10°C. The pellet was washed with cold 80% ethanol. The precipitated proteins were resuspended in PBS, incubated for 10 min at 37°C, and kept at -20°C until use.

*Antibody generation using recombinant proteins.* Seven male mice and 7 guinea pigs were used, considering the correspondent norm (14-2017, 2017). The animals were inoculated three times, subcutaneously every 15 days with the recombinant proteins (15,9 mg/ml in 1 ml for guinea pigs and 0.3 ml for mice), in a Freund's complete adjuvant emulsion mixed with FIS peptide (FISEAAIIHVLHSR; 0.5 mg/ml) as immunomodulating agent (Prieto *et al.*, 1995).

*Transfection of MA104 cell line.* MA104 cells were grown in MEM medium supplemented with 10% fetal bovine serum (FBS), up to 80% confluence. In concentrations of 0, 1, 1.5, and 5  $\mu$ g/ml, the plasmids were incubated with Hexadimethrine bromide (PolybreneR; 6  $\mu$ g/ml) for 15 min at 37°C, and added to the MA104 cells. The transfected cells were cultivated for 24, 36, and 48 h at 37°C in 5% CO<sub>2</sub>. The protein expression in the MA104 cells was evaluated by epifluorescence as previously described (Gómez *et al.*, 2016). Ten representative photographs were taken per plate, and the semi-quantitative fluorescence analysis was carried out using the software Image J 1.44 Java 1.6.0\_20 of 32 bits; plugins (analyze, measure), calculating the corrected total cell fluorescence (CTCF).

*Cell and viral recombinant protein binding assays.* To evaluate the interaction in MA104 cells transfected with different plasmids, four assays were performed. 1. *Co-transfection:* MA104 cells were independently co-transfected with plasmids that express each of the NSPs (pcDNA3.1 Hygro(-) NSP2, pcDNA3.1 Hygro(-) NSP4, pcDNA3.1 Hygro(-) NSP5, pcDNA4 Myc NSP3, pCR-flag NSP1), and each of the plasmids that express cellular proteins (pcDNA flag PPAR gamma, p50 cFlag pcDNA3, pcDNA flag PGC1 (180-797), pCRFlagIKKalpha, pcDNA4 myc PGC1 alpha) at a 2  $\mu$ g/ml concentration, and cultivated for 36 hours post-transfection (h.p.t) at 37°C with 5% CO<sub>2</sub>. As a control, MA104 cells were transfected with the plasmids that individually express each of the NSPs. To evaluate the binding, the cells were lysed with RIPA buffer. The lysate was added to an ELISA plate previously incubated with an anti-NSPs hyperimmune serum (1:1000) generated in guinea pig or mouse in our laboratory, and as the primary antibody, antibodies against Myc and Flag tags at a concentration of 2  $\mu$ g/ml each. As a negative control, the absorbance of the non-infected or non-transfected MA104 cell lysates was used; likewise, the lysates of cells transfected with empty vector. Another control was cell lysate from cells transfected with the plasmids that express each NSPs individually, without co-transfection. The positive binding control was the lysate of cells co-transfected with plasmids that express viral proteins NSP2+NSP5 and cellular proteins PPAR $\gamma$ +RXR, PPAR $\gamma$ +PGC1, and PPAR $\gamma$ +NF $\kappa$ B. 2. *Infection and transfection:* MA104 cells were transfected with each of the plasmids that express cellular proteins pcDNA Flag PPAR gamma, p50 cFlag pcDNA3, pcDNA flag PGC1 (180-797), pCR-Flag-IKKalpha, and pcDNA4 myc PGC1 alpha at a 2  $\mu$ g/ml concentration and cultivated for 36 h, at 37°C with 5% CO<sub>2</sub>. Meanwhile, these cells were infected with rotavirus RRV with MOI of 0.8 and cultivated for 12 h at 37°C with 5% CO<sub>2</sub>. As a control, cells transfected with empty plasmids were used. The cells were lysed and added to an ELISA plate according to the procedure described previously. As a negative control, non-infected, non-transfected MA104 cells and the lysates of cells transfected with empty vector were used. As a positive binding control, the lysate of cells co-transfected with the NSP2+NSP5 plasmids or infected and/or co-transfected with plasmids that express cellular proteins PPAR $\gamma$ +RXR or PPAR $\gamma$ +PGC1 or PPAR $\gamma$ +NF $\kappa$ B were used. 3. *Transfection of NSPs:* to analyze the binding between the rNSPs and the cellular proteins, the MA104 were transfected with plasmids that express each of the NSPs (2  $\mu$ g/ml), and were cultivated for 36 h at 37°C with 5% CO<sub>2</sub>. The cells were lysed and the lysates were analyzed using the ELISA, as described above. As a capture antibody anti-NSPs were used and as the primary antibody, antibodies against each of the cellular proteins PPAR $\gamma$ , Peroxisome proliferator-activated receptor gamma coactivator 1-alpha (PGC1 $\alpha$ ), RXR, and p-IKK and p-NF $\kappa$ B. As a negative control, the non-infected, non-transfected MA104 cells lysate and the lysates of cells transfected with empty vector were used. As a positive control of the binding, the lysate of cells co-transfected with plasmids

NSP2+NSP5, PPAR $\gamma$ +RXR, PPAR $\gamma$ +PGC1, or PPAR $\gamma$ +NF $\kappa$ B were analyzed. 4. *RRV infection (MOI 0.8)*: Cells MA104 were infected with rotavirus for 12 h and to determine the expression of viral and cellular proteins the cells were lysed and analyzed by ELISA as described above. As a capture antibody, anti-NSPs were used and as the primary antibody, antibodies against each of the cellular proteins PPAR $\gamma$ , PGC1, RXR, p-IKK, and p-NF $\kappa$ B (200  $\mu$ g/ml) were used. As a negative control, the non-infected, non-transfected MA104 cell lysates and the lysates of cells transfected with empty vector were used. As a positive control of interaction, infected cell lysates were analyzed, and the binding between NSP2+NSP5, PPAR $\gamma$ +RXR, PPAR $\gamma$ +PGC1, or PPAR $\gamma$ +NF $\kappa$ B was detected.

*Agonists and inhibitors of PPAR $\gamma$  and NF $\kappa$ B.* To analyze the expression of the PPAR $\gamma$  and NF $\kappa$ B proteins in cells infected with RRV, the cells were infected with MOI 0.8, incubated for 1 h at 37°C, washed with medium without SFB, and 153 mM TZD, 10  $\mu$ M PPAR $\gamma$ -GW9662, or 100  $\mu$ M curcumin (CUR) was added. The cells were cultivated for 12 h at 37°C and 5% CO<sub>2</sub>. As a control, non-transfected cells and cells transfected with plasmids that express each of the NSPs treated with a TZD, CUR, or GW9662 were used. To localize the expression of PPAR $\gamma$  in the cytoplasm and the nucleus, nuclear extraction in uninfected and infected cells was carried out, following the technique described by Abcam (Abcam, 2020). The nuclei were evaluated through the epifluorescence, analyzing the actin proteins as cytoplasmic control and PGC1 $\alpha$  as nuclear control. The presence of PPAR $\gamma$  and p-PPAR $\gamma$  in nucleus and cytoplasm was detected in Western blot, differentiating them by molecular weight. The binding of PPAR $\gamma$  with PGC1 $\alpha$  in nucleus was detected through the capture-ELISA technique. For this purpose, the cells were lysed, and the lysates were added to an ELISA plate previously incubated with anti-PPAR $\gamma$  hyperimmune serum (1:1000). As the primary antibody, an anti-PGC1 $\alpha$  antibody generated in goat was used (200  $\mu$ g/ml), and as secondary antibody, anti-goat conjugated with IgG- HRP (0.08  $\mu$ g/ml). As a negative control, non-infected and non-transfected MA104 cell lysates and the lysate of MA104 cells non-infected and transfected with an empty vector, were used.

*ELISA and flow cytometry.* Capture ELISA was conducted as previously described (Gómez *et al.*, 2016); as capture antibodies, hyperimmune sera generated in guinea pig or mouse were used. These sera are reactive with rotavirus nonstructural proteins diluted 1:1000 in 50  $\mu$ l of PBS. A quantity of 74.62 mg/ml of the total protein of each of the NSPs recombinant proteins or cell lysates of MA104 transfected or non-transfected cells were added at each well. As primary antibodies anti-PPAR $\gamma$ , -PGC1 $\alpha$ , -IKK-p, -IKK, -I $\kappa$ B, -NF $\kappa$ B-p, or -NF $\kappa$ B (0.2  $\mu$ g/ml in PBS) were used.

Direct ELISA was conducted as previously described (Gómez *et al.*, 2016), 74.62 mg/ml of the cell lysate was added to each well. As primary antibodies anti-PPAR $\gamma$ , -PGC1 $\alpha$ , -IKK-p, -IKK, -I $\kappa$ B, -NF $\kappa$ B-p, or -NF $\kappa$ B (0.2  $\mu$ g/ml in PBS) were used. The ELISA plates were read at 490 nm in an ELISA Stat Fax 303/

Plus reader (Awareness Technology, Inc.). Flow cytometry was conducted as previously described (Gómez *et al.*, 2016).

*Luciferase assay.* The cells co-transfected with eukaryotic expression plasmids NSPs and PPRE X3 TK luc (Addgene, USA) or NF $\kappa$ B luc, (Addgene) were lysed with lysis buffer (50 mM Tris, 100 mM NaCl, 5 mM MgCl<sub>2</sub>, 1% Triton X-100, 50% glycerol and protease inhibitor (PMSF)) and were incubated for 20 min at room temperature. Subsequently, the protocol of the Gaussia Luciferase kit (BioLabs®, USA) was followed. The reading was performed in BioTek FLX800TB fluorometer equipment (BioTek Instruments, Inc, USA).

*Epifluorescence and confocal microscopy.* Epifluorescence and confocal microscopy in transfected cells were conducted as previously described (Gómez *et al.*, 2016). As primary antibodies, hyperimmune anti-NSPs serum generated in mouse or guinea pig (1:1000) and/or polyclonal antibody anti-PPAR $\gamma$ , PGC1 $\alpha$ , IKK-p, IKK, -I $\kappa$ B, NF $\kappa$ B-p, were added. As secondary antibody, anti-rabbit, goat or guinea pig conjugated with FITC-Texas red and DAPI were added. The images were taken on an epifluorescence microscope SOPTOP (Sunny Optical Technology, China). The confocal microscopy was performed on an Olympus FV1000 microscope and was analyzed with the Image J (Fiji) program (Schindelin *et al.*, 2012). To carry out the superposition and co-localization analysis, three coefficients, Pearson's, Overlap divided into two overlap coefficients, k1 and k2, and Mander's, were calculated in the program Image J-JaCoP (Bolte and Cordelières, 2006).

*Statistics.* All the experiments were performed in duplicate or triplicate. The data analysis was performed employing one-way ANOVA (analysis of variance) with a Dunnett's test (comparison between groups against a control group) level of significance alpha of  $p < 0.05$  defined as significant with a confidence interval of 95%.

## Results and Discussion

### *Standardization of the transfection efficiency*

The plasmid concentrations and the time-points of cell culture at which proteins of interest were expressed were not affecting cell viability. Cells containing 2  $\mu$ g/ml of plasmid and cultivated for 36 h, had plasmid protein expression similar to the expression of the rotavirus RRV infected cells (MOI = 0.8) cultivated for 12 h. Also, the expression in cells transfected with 5  $\mu$ g/ml of plasmid cultivated for 36 h, was similar, but the viability was lower, which is why 2  $\mu$ g/ml of plasmid were used during the whole study (data not shown). Total corrected NSPs fluorescence was calculated in the cells transfected with 2  $\mu$ g/ml of plasmid and cultivated for 36 h.p.t. and compared with cells infected with RRV 12 h.p.i. and comparable values were observed between the transfected and

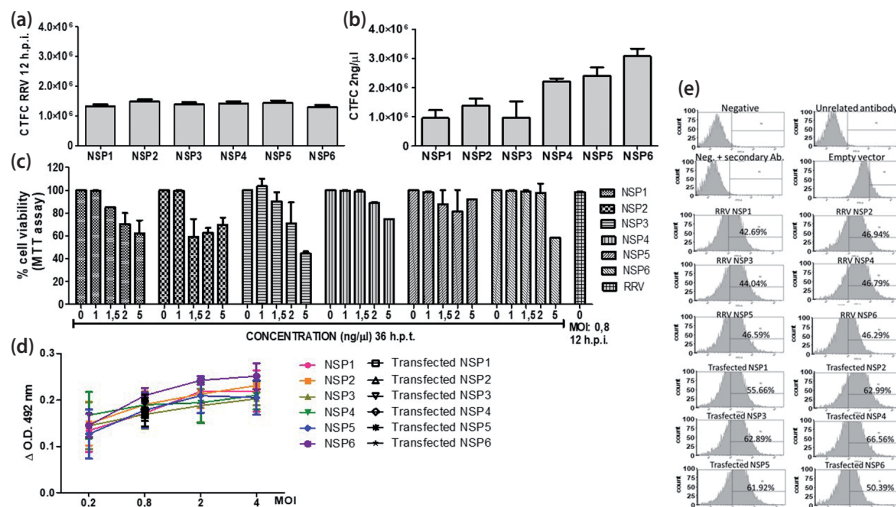


Fig. 1

#### Standardization of the transfection efficiency

Corrected total cell fluorescence of each protein in MA104 infected and transfected cells (a, b). Cell viability analyzed by the MTT assay in cells transfected with different plasmid concentrations (c). Capture ELISA. Expression of each NSPs in infected cells at different MOI and in cells transfected with 2  $\mu$ g/ml of each plasmid 36 h.p.t (d). Flow cytometry of the NSPs protein in MA104 infected and transfected cells (e).

infected cells (Fig. 1a,b). Cell viability was determined at different hours post-transfection using the MTT assay (Fig. 1c). After 36 h.p.t. the viability of transfected cells was 75%–80% for the 2  $\mu$ g/ml of plasmid and of 60%–70% for 5  $\mu$ g/ml of plasmid; in the transfected cells cultivated 48 h.p.t., viability was 60%–70% with a 2  $\mu$ g/ml concentration (data not shown). By means of the capture ELISA and flow cytometry, the expression of the NSPs in the RRV infected cells was measured at different MOI (0.2, 0.8, 2 and 4), and in cells transfected with the 2  $\mu$ g/ml of plasmids that express the NSPs cultivated 36 h.p.t. (Fig. 1d,e). It was observed that in cells transfected with the plasmids, the tendency in the expression of all the NSPs is like the one obtained for the NSPs in RRV infected cells (MOI of 0.8). The results presented are the average of the two experiments.

#### The RRV infection alters the expression of proteins related to the NF $\kappa$ B and PPAR $\gamma$ pathway in MA104 cells

The expression of cellular proteins IKK $\alpha/\beta$ , p-IKK $\alpha/\beta$ , I $\kappa$ B, NF $\kappa$ B, p-NF $\kappa$ B, PPAR $\gamma$ , PGC1 $\alpha$ , RXR in MA104 cells transfected with plasmids that express NSPs proteins was analyzed by ELISA. The non-infected and non-transfected MA104 cells and non-infected and transfected with empty vector pcDNA 3.1 Hygro (+) cells were used as negative control. The expression was compared with the RRV infected cells.

ELISA analysis showed that the IKK  $\alpha/\beta$  and I $\kappa$ B proteins do not show any differences in expression among

non-infected cells and rotavirus infected cells or the cells transfected with each of the NSPs (data not shown). However, the phosphorylated p-IKK  $\alpha/\beta$  protein showed a significant increase in expression in rotavirus infected cells and cells transfected with NSP3, NSP4, NSP5, and NSP6 compared to the negative control.

The absorbance of p-IKK  $\alpha/\beta$  in infected cells was similar to those transfected with NSP3, NSP4 and NSP5, with the lowest absorbance in NSP6. The absorbance of NF $\kappa$ B in rotavirus RRV infected cells was similar to those transfected with NSP1, with lower absorbance in NSP3 and NSP4, and with a significant increase in expression, regarding the negative control. The absorbance of NF $\kappa$ B phosphorylated protein (p-NF $\kappa$ B) in rotavirus infected cells was higher than in cells transfected with NSP1, NSP2, NSP3, NSP4, NSP5, and NSP6, but with a significant increase in expression compared to the negative control (Fig. 2a). For luminescence analysis, RRV infected cells were transfected with the NF $\kappa$ B-Luc plasmid (2  $\mu$ g/ml). Similarly, cells transfected with plasmids that express each of the NSPs were co-transfected with NF $\kappa$ B-Luc (2  $\mu$ g/ml, 1:1). As a control, uninfected cells were transfected with the NF $\kappa$ B-Luc plasmid (2  $\mu$ g/ml). It was observed that in rotavirus infected cells, the luminescence of NF $\kappa$ B-Luc was 225.75 Relative Light Unit (RLU), and in uninfected cells was 72.87 RLU, suggesting that the RRV infection induces an increase in the promoter activity. The luminescence in the co-transfected cells (NF $\kappa$ B-Luc-NSPs, 1:1, 2  $\mu$ g/ml) in NSP4 was 178.8 RLU, and in NSP6 178.33 RLU. The rest of the NSPs did not present any changes in

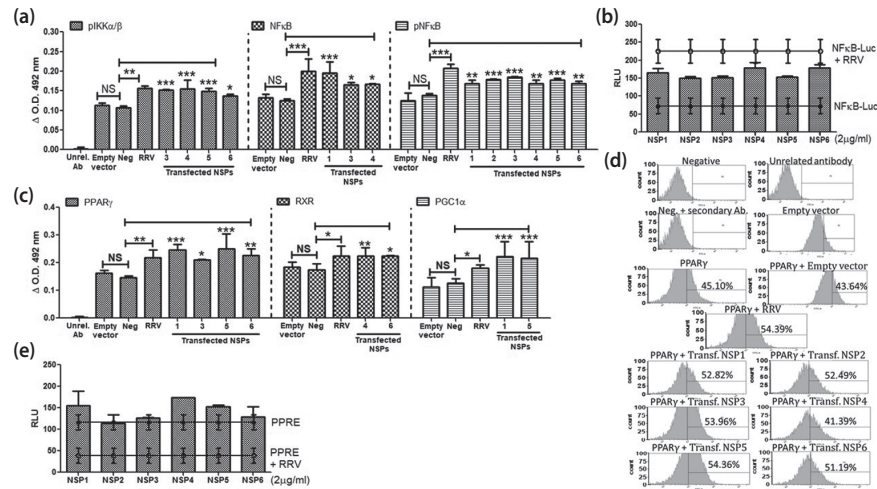


Fig. 2

### The RRV infection alters the expression of proteins related to the NF $\kappa$ B and PPAR $\gamma$ pathway

ELISA of the expression of p-IKK $\alpha/\beta$ , NF $\kappa$ B and p-NF $\kappa$ B proteins in MA104 cells transfected with plasmids expressing NSPs of RRV (a). Luminescence of the transcriptional activity of the NF $\kappa$ B promoter in MA104 cells co-transfected with plasmids expressing RRV at different concentrations of 2 ng/ $\mu$ l and NF $\kappa$ B-Luc 2 ng/ $\mu$ l of plasmid (b). ELISA of the expression of PPAR $\gamma$ , RXR and PGC1 $\alpha$  proteins in MA104 cells transfected with plasmids expressing NSPs of RRV (c). Flow cytometry of the expression of PPAR $\gamma$  protein in MA104 infected and transfected cells (d). Luminescence of the PPRE transcriptional activity in MA104 cells co-transfected with plasmids expressing RRV at different concentrations of 2 ng/ $\mu$ l and PPRE-luc 2 ng/ $\mu$ l of plasmid (e).

comparison with the uninfected cells transfected with the NF $\kappa$ B-Luc. These results suggest that RRV activates the NF $\kappa$ B inflammatory pathway when increasing the phosphorylated portion of p-IKK and p-NF $\kappa$ B. Similarly, p-IKK is increased when transfected with NSP1, 3, 4, 5, and 6. Additionally, the NF $\kappa$ B promoter activity is stimulated in cells infected with rotavirus or transfected with NSP4 and NSP5. Other research has observed that some viruses modify the NF $\kappa$ B expression to alter the cellular mechanisms to eliminate the infection (Deng *et al.*, 2018; Zhao *et al.*, 2015; Kumar *et al.*, 2008). The current pandemic virus, SARS-CoV-2, regulates the NF $\kappa$ B signaling pathway positively (Huang *et al.*, 2020; Lauxmann *et al.*, 2020; Li *et al.*, 2020) (Fig. 2b). In analyzing the PPAR $\gamma$  protein by capture ELISA, the absorbance in RRV infected cells was of  $0.219 \pm 0.049$ , and in cells transfected with NSP1,  $0.245 \pm 0.029$ , NSP3,  $0.210 \pm 0.003$ , NSP5,  $0.249 \pm 0.077$ , and NSP6,  $0.227 \pm 0.033$  with significant increase in comparison with non-infected cells. In analyzing the PGC1 $\alpha$  protein by direct ELISA, in rotavirus infected cells, the absorbance was  $0.179 \pm 0.025$  and in cells transfected with NSP1,  $0.221 \pm 0.077$ , and NSP5,  $0.216 \pm 0.086$  with a significant increase in expression in comparison with non-infected cells. In analyzing the RXR protein in RRV infected cells by direct ELISA the absorbance was  $0.224 \pm 0.061$ , and in cells transfected with NSP4,  $0.225 \pm 0.042$ , and NSP6,  $0.224 \pm 0.003$  with a significant increase in expression in comparison with non-infected cells (Fig. 2c). In analysis by flow cytometry in comparison with non-infected cells,

PPAR $\gamma$  expression in cells infected with rotavirus was 54.39%. It also increased in cells transfected with NSP1, 52.82%, NSP2, 52.49%, NSP3, 53.96%, NSP5, 54.36%, and NSP6, 51.19% (Fig. 2d). The PPRE promoter activity was analyzed through the luminescence technique in RRV infected cells, and in cells transfected with 2  $\mu$ g/ml of the PPRE plasmid, and also in the cells transfected with the plasmids expressing each of the NSPs and co-transfected with the PPRE plasmid (2  $\mu$ g/ml). As a negative control, uninfected cells were transfected with PPRE plasmid (2  $\mu$ g/ml). The luminescence was 38.4 RLU when cells were infected with rotavirus, while without RRV infection it was 116.02 RLU, a decrease being observed in infected cells compared to uninfected cells. In contrast, no changes were observed in the luminescence expression in the co-transfected (PPRE-NSPs) cells, in comparison with the non-infected transfected cells (Fig. 2e). These results suggest that RRV inhibits the anti-inflammatory pathway. Paradoxically, RRV infection also increases the proportion of proteins related to the PPAR $\gamma$ , PGC1, and RXR anti-inflammatory pathway, thus decreasing the PPRE transcriptional activity. Various investigations have reported that different viruses modify PPAR $\gamma$  expression, for example, the human cytomegalovirus (HCMV) induces PPAR $\gamma$  transcriptional activity in infected cells, demonstrating that when activating PPAR $\gamma$ , the production of the virus is dramatically impaired, and the early human trophoblast migration and invasion is drastically affected (Rauwel *et al.*, 2010). The influenza A virus (IAV)

**Table 1. Analysis with recombinant protein (binding)**

Classification	Groups	Concentrations ( $\mu$ g/ml) absorbance $\pm$ SD			
		1.56	3.13	60	400
Positive binding control	rNSP2-rNSP5	0.187 $\pm$ 0.083	0.243 $\pm$ 0.048	0.286 $\pm$ 0.062	0.498 $\pm$ 0.052
	rPPAR $\gamma$ -rRXR	0.188 $\pm$ 0.082	0.212 $\pm$ 0.072	0.333 $\pm$ 0.044	0.465 $\pm$ 0.068
Negative control	rPPAR $\gamma$	0.116 $\pm$ 0.005	0.146 $\pm$ 0.048	0.300 $\pm$ 0.122	0.428 $\pm$ 0.172
	rRXR	0.061 $\pm$ 0.001	0.197 $\pm$ 0.035	0.229 $\pm$ 0.030	0.403 $\pm$ 0.074
	rNSP1	0.081 $\pm$ 0.004	0.131 $\pm$ 0.033	0.227 $\pm$ 0.016	0.516 $\pm$ 0.177
	rNSP2	0.047 $\pm$ 0.003	0.054 $\pm$ 0.001	0.201 $\pm$ 0.051	0.511 $\pm$ 0.123
	rNSP3	0.080 $\pm$ 0.050	0.099 $\pm$ 0.059	0.175 $\pm$ 0.005	0.594 $\pm$ 0.114
	rNSP4	0.062 $\pm$ 0.019	0.075 $\pm$ 0.037	0.227 $\pm$ 0.075	0.417 $\pm$ 0.109
	rPPAR $\gamma$ -rNSP1	0.097 $\pm$ 0.001	0.414 $\pm$ 0.078	0.447 $\pm$ 0.038	0.642 $\pm$ 0.061
Protein binding	rPPAR $\gamma$ -rNSP2	0.289 $\pm$ 0.053	0.371 $\pm$ 0.033	0.484 $\pm$ 0.001	0.527 $\pm$ 0.079
	rPPAR $\gamma$ -rNSP3	0.187 $\pm$ 0.083	0.243 $\pm$ 0.048	0.286 $\pm$ 0.062	0.498 $\pm$ 0.052
	rPPAR $\gamma$ -rNSP4	0.188 $\pm$ 0.082	0.212 $\pm$ 0.072	0.333 $\pm$ 0.044	0.465 $\pm$ 0.068
	rRXR-rNSP1	0.123 $\pm$ 0.080	0.126 $\pm$ 0.085	0.211 $\pm$ 0.029	0.371 $\pm$ 0.103

Evaluation criterion: The absorbance values of the mixture of recombinant cellular and viral proteins greater than or equal to those obtained in negative control were considered positive for the binding (in 2 or more concentrations).

regulates PPAR $\gamma$  negatively, after the infection of alveolar macrophages (AM), through type IFN-I dependent signaling. Similarly, the PPAR $\gamma$  expression in AM suppresses the exaggerated antiviral and inflammatory response of AM after infections by IAV and respiratory syncytial virus (Huang *et al.*, 2019).

#### *Formation of protein complexes between rotavirus nonstructural proteins and proteins related to PPAR $\gamma$ -NF $\kappa$ B pathways*

To determine the formation of complexes between the RRV NSPs and the proteins related to the NF $\kappa$ B pathway (IKK $\alpha$ , p-IKK $\alpha$ / $\beta$ , NF $\kappa$ B p50, and p-NF $\kappa$ B) and PPAR $\gamma$  pathway (PPAR $\gamma$ , PGC1 $\alpha$ , and RXR), binding between recombinant cellular and viral proteins was analyzed through capture ELISA assays, immunofluorescence and confocal microscopy.

For the analysis of recombinant protein, each of the recombinant soluble proteins (rPPAR $\gamma$ , rRXR, and rPGC1) was mixed with each of the rNSPs at different concentrations. The absorbance obtained in the mixture of rNSPs recombinant proteins and recombinant cellular proteins rPPAR $\gamma$ , rRXR, and rPGC1 was compared with the absorbance of the rNSPs proteins and cellular proteins individually. As an acceptance criterion, it was proposed that the absorbance values of the mixture of recombinant cellular and viral proteins greater than or equal to those obtained in negative control were considered positive for the binding

(in 2 or more concentrations). In this way, the binding between rNSP1 with rPPAR $\gamma$  and rRXR in the concentrations of 1.56, 3.13, 60, and 400  $\mu$ g/ml, respectively was observed. The rNSP5 protein did not show any interaction with the recombinant cellular proteins evaluated (Table 1).

In the analysis of transfected cells, as an acceptance criterion was considered positive for binding when the absorbance value in the infection model was significant ( $p < 0.05$ ) in comparison with the non-infected, nor transfected cells, and coincides with the other evaluation models (co-transfection, transfection-infection, and transfection). Here, we show that PPAR $\gamma$  binds to NSP1, 2, 3, and 4; RXR binds to NSP1 and 2; p-IKK binds to NSP 1, 2, 3, 4, 5, 6; p-NF $\kappa$ B binds to NSP 5 and 6. These results were observed in both analysis (Table 2).

#### *Colocalization between rotavirus nonstructural proteins and proteins related to PPAR $\gamma$ -NF $\kappa$ B pathway*

Before performing the colocalization through the confocal technique, screening using epifluorescence technique was performed to determine if the rotavirus NSPs that were positive for binding in the ELISA overlap with cellular proteins related to PPAR $\gamma$  and NF $\kappa$ B pathways. MA104 cells were transfected with each of the plasmids that express NSPs, and the expression of each viral protein with each cellular protein (RXR, PGC1, PPAR $\gamma$ , p-IKK $\alpha$ / $\beta$ , and NF $\kappa$ B) was analyzed by antibodies. The images taken from each group were analyzed using the program Image

Table 2. Co-localization in MA104 cells

Classification	Groups	Absorbance $\pm$ SD			
		Co-transfected	Transfected	Infected RRV + transfected	Infected RRV
Positive binding control	NSP2-NSP5		0.235 $\pm$ 0.022		0.276 $\pm$ 0.040
	PPAR $\gamma$ -RXR	0.153 $\pm$ 0.018	0.211 $\pm$ 0.009	0.435 $\pm$ 0.099	0.297 $\pm$ 0.039
	PPAR $\gamma$		0.145 $\pm$ 0.006		0.202 $\pm$ 0.013
	RXR		0.182 $\pm$ 0.030		0.196 $\pm$ 0.024
	p-IKK $\alpha$ / $\beta$		0.202 $\pm$ 0.017		0.199 $\pm$ 0.020
	p-NF $\kappa$ B		0.149 $\pm$ 0.021		0.204 $\pm$ 0.021
Negative control	NSP1		0.145 $\pm$ 0.016		0.127 $\pm$ 0.005
	NSP2		0.146 $\pm$ 0.017		0.122 $\pm$ 0.004
	NSP3		0.155 $\pm$ 0.0231		0.135 $\pm$ 0.014
	NSP4		0.146 $\pm$ 0.015		0.142 $\pm$ 0.010
	NSP5		0.157 $\pm$ 0.014		0.147 $\pm$ 0.004
	NSP6		0.137 $\pm$ 0.001		0.126 $\pm$ 0.018
Protein binding	PPAR $\gamma$ -NSP1	0.208 $\pm$ 0.037 (NS)	0.155 $\pm$ 0.004 (NS)	0.230 $\pm$ 0.049 (*)	0.201 $\pm$ 0.017 (*)
	PPAR $\gamma$ -NSP2	0.164 $\pm$ 0.021 (NS)	0.143 $\pm$ 0.002 (NS)	0.240 $\pm$ 0.054 (**)	0.187 $\pm$ 0.014 (*)
	PPAR $\gamma$ -NSP3	0.162 $\pm$ 0.016 (NS)	0.154 $\pm$ 0.007 (NS)	0.228 $\pm$ 0.048 (*)	0.216 $\pm$ 0.015 (*)
	PPAR $\gamma$ -NSP4	0.183 $\pm$ 0.037 (NS)	0.162 $\pm$ 0.012 (NS)	0.236 $\pm$ 0.049 (*)	0.214 $\pm$ 0.017 (**)
	RXR-NSP1		0.170 $\pm$ 0.012 (NS)		0.205 $\pm$ 0.021 (*)
	RXR-NSP6		0.218 $\pm$ 0.031 (***)		0.205 $\pm$ 0.021 (*)
	p-IKK $\alpha$ / $\beta$ -NSP1	0.294 $\pm$ 0.095 (*)	0.198 $\pm$ 0.014 (*)	0.201 $\pm$ 0.036 (NS)	0.217 $\pm$ 0.023 (*)
	p-IKK $\alpha$ / $\beta$ -NSP2	0.242 $\pm$ 0.057 (*)	0.201 $\pm$ 0.024 (**)	0.211 $\pm$ 0.037 (NS)	0.208 $\pm$ 0.023 (*)
	p-IKK $\alpha$ / $\beta$ -NSP3	0.201 $\pm$ 0.030 (NS)	0.212 $\pm$ 0.031 (**)	0.196 $\pm$ 0.035 (NS)	0.213 $\pm$ 0.023 (*)
	p-IKK $\alpha$ / $\beta$ -NSP4	0.212 $\pm$ 0.038 (*)	0.206 $\pm$ 0.027 (***)	0.205 $\pm$ 0.036 (NS)	0.204 $\pm$ 0.028 (*)
	p-IKK $\alpha$ / $\beta$ -NSP5	0.234 $\pm$ 0.052 (**)	0.205 $\pm$ 0.025 (*)	0.186 $\pm$ 0.037 (NS)	0.223 $\pm$ 0.024 (**)
	p-IKK $\alpha$ / $\beta$ -NSP6	0.293 $\pm$ 0.063 (**)	0.183 $\pm$ 0.032 (*)	0.251 $\pm$ 0.023 (**)	0.206 $\pm$ 0.027 (*)
	p-NF $\kappa$ B- NSP5	0.221 $\pm$ 0.038 (*)	0.184 $\pm$ 0.025 (NS)	0.160 $\pm$ 0.028 (NS)	0.211 $\pm$ 0.019 (*)
	p-NF $\kappa$ B- NSP6	0.271 $\pm$ 0.058 (*)	0.156 $\pm$ 0.008 (NS)	0.187 $\pm$ 0.003 (NS)	0.201 $\pm$ 0.021 (*)

Acceptance criterion: It is considered as positive for binding when the absorbance value at the joints of the infection is significant and coincides with the other evaluation models (co-transfection; transfection; and infection and transfection). Statistical analysis was performed by one-way Anova and Dunnett's multiple comparison test (Comparison of NSPs and binding groups).

J-JaCoP to calculate protein colocalization (Fig. 3a-f). The expression of viral and cellular proteins in non-infected nor transfected MA104 cells was used as a negative control. As transfection control, MA104 cells were transfected with an empty vector. As a positive control, the colocalization in cells co-transfected with NSP2-NSP5 and rotavirus infected cells (MOI 0.8) 12 h.p.i. (Zhao *et al.*, 2015) was used. The coefficients calculated in transfected cells were compared, considering as positive colocalization all the values greater than or equal to Pearson's and Overlap coefficients reported in the positive control. In the positive controls (NSP2+NSP5 co-transfected), the Pearson's coefficient was 0.94, the Overlap coefficient was 0.939, and

in RRV infected cells was 0.944, 0.939, respectively (Fig. 3a, Table 3). Considering the previous coefficients, when evaluating the cellular proteins, it was found that they colocalize as follows: RXR with NSP1, NSP2, and NSP4, with Pearson's coefficient 0.962, 0.960, 0.954, and Overlap coefficient 0.969, 0.975, and 0.950, respectively (Fig. 3b, Table 3). PPAR $\gamma$  colocalizes with NSP1, NSP2, NSP3, and NSP4; with Pearson's coefficient 0.963, 0.960, 0.977, 0.947, and Overlap coefficient 0.962, 0.961, 0.985 and 0.968, respectively (Fig. 3c, Table 3). PGC1 did not present any colocalization with any of the NSPs proteins (Fig. 3d, Table 3). p-IKK $\alpha$ / $\beta$  showed colocalization with NSP2, NSP3, and NSP6, with Pearson's coefficient 0.982, 0.969, 0.985, and Overlap coef-

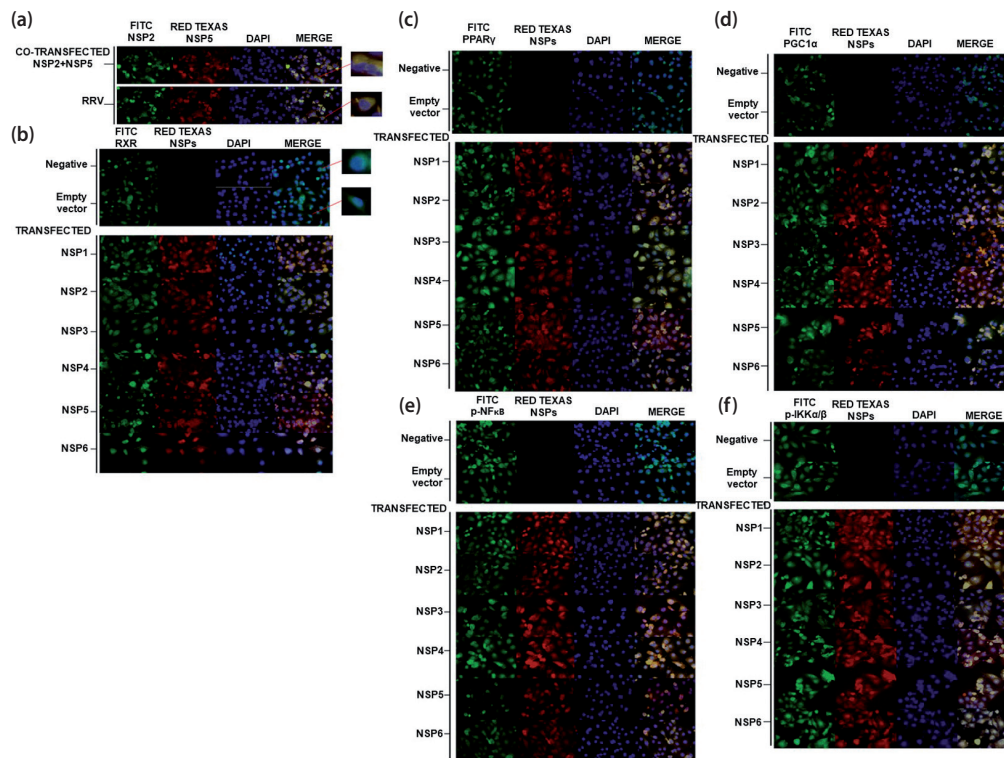


Fig. 3

### Epi-immunofluorescence

(a-f) Representative images of RXR, PGC1 $\alpha$ , PPAR $\gamma$ , p-IKK $\alpha/\beta$  and p-NF $\kappa$ B proteins of the expression and magnification of the merge of the images of the positive, negative controls and empty vector.

efficient 0.965, 0.973, and 0.987, respectively (Fig. 3e, Table 3). p-NF $\kappa$ B colocalized with NSP2 with Pearson's coefficient 0.915 and Overlap coefficient 0.946 (Fig. 3f, Table 3).

To determine if there is co-localization between viral and cellular proteins, through the confocal microscopy technique and image analysis by the program Image J, MA104 cells were transfected with each of the plasmids that express viral proteins (NSPs1-6). Through specific antibodies, the expression of viral and cellular proteins (RXR, PPAR $\gamma$ , p-IKK $\alpha/\beta$ , and NF $\kappa$ B) was detected. Subsequently, some images were taken with the Olympus FV1000 confocal laser scanning microscope, with optical sectioning of the samples in Z plane (depth plane) with a thickness of 2  $\mu$ m, obtaining 27 images for each analyzed group (Fig. 4a-f). The protein colocalization calculation analysis was performed using the program Image J-JaCoP, calculating the Pearson's, Overlap, and Mander's coefficients. As a negative control, viral and cellular proteins in non-infected and non-transfected MA104 cells were detected. As a transfection control, non-infected MA104 cells transfected with empty vectors were used. As a positive control, the colocalization was detected between NSP2+NSP5 in co-transfected MA104 cells and MA104 rotavirus infected cells with an MOI of 0.8

12 h.p.i. (Rainsford and Malcolm, 2007). The Pearson's and Overlap coefficients in the positive controls (NSP2+NSP5 co-transfected) were 0.430, 0.572, and in the RRV infected cells were 0.499 and 0.546, respectively (Fig. 4a, Table 4). Considering the previous coefficients, when evaluating the cellular proteins, it was found that RXR colocalized with NSP1, with Pearson's coefficient 0.436 and Overlap coefficient 0.549 (Fig. 4b, Table 4). PPAR $\gamma$  colocalized with NSP1 and NSP3, with Pearson's coefficient 0.505, 0.542, and Overlap coefficient 0.519, 0.545, respectively (Fig. 4c, Table 4). p-IKK $\alpha/\beta$  colocalized with NSP2, with Pearson's coefficient 0.548, and Overlap coefficient 0.614 (Fig. 4d, Table 4). p-NF $\kappa$ B colocalized with NSP5, with Pearson's coefficient 0.715 and Overlap coefficient 0.725 (Fig. 4e, Table 4). Our work evaluated the binding between recombinant cellular proteins PPAR $\gamma$ , RXR, PGC1 $\alpha$ , and recombinant viral proteins NSP1, NSP2, NSP3, NSP4, NSP5. Binding between PPAR $\gamma$  with NSP1, NSP2, NSP3, NSP4, and RXR with NSP1 was found. Similarly, the binding in MA104 cells was evaluated, finding that there is interaction between PPAR $\gamma$  with NSP1, NSP2, NSP3, NSP4; RXR with NSP1, NSP6; p-IKK with NSP1, NSP2, NSP3, NSP4, NSP5, NSP6, and p-NF $\kappa$ B with NSP5, NSP6 12 h.p.i. This finding was supported with the results obtained through

**Table 3. Co-localization of rotavirus nonstructural proteins and proteins related to PPAR $\gamma$ -NF $\kappa$ B pathway**

Sample	Positive control			
	Pearson's coefficient	Overlap coefficient	Manders' coefficients	
Co-transfected NSP2+NSP5	0.941	0.939	M1=0.969	M2=0.999
RRV	0.944	0.939	M1=0.898	M2=0.999
RXR				
Negative control	0.578	0.652	M1=0.994	M2=0.565
Empty vector	0.345	0.572	M1=0.998	M2=0.517
NSP1	0.962	0.969	M1=0.856	M2=0.991
NSP2	0.96	0.975	M1=0.997	M2=0.985
NSP4	0.954	0.95	M1=0.98	M2=0.999
PPAR $\gamma$				
Negative control	0.159	0.159	M1=1.0	M2=0.0080
Empty vector	0.393	0.381	M1=1.0	M2=0.075
NSP1	0.963	0.962	M1=0.938	M2=0.999
NSP2	0.96	0.961	M1=0.93	M2=0.999
NSP3	0.977	0.985	M1=0.998	M2=0.986
NSP4	0.947	0.968	M1=0.995	M2=0.981
p-NF $\kappa$ B				
Negative control	0.183	0.188	M1=0.977	M2=0.057
Empty vector	0.0070	0.0080	M1=0.902	M2=0.0
NSP2	0.915	0.946	M1=0.961	M2=0.943
p-IKK $\alpha/\beta$				
Negative control	0.096	0.613	M1=1.0	M2=0.58
Empty vector	0.159	0.482	M1=1.0	M2=0.418
NSP2	0.982	0.965	M1=0.962	M2=1.000
NSP3	0.969	0.973	M1=0.964	M2=0.999
NSP6	0.985	0.987	M1=0.979	M2=0.999

image overlapping of PPAR $\gamma$  cellular proteins with NSP1, NSP2, NSP3, and NSP4; RXR with NSP1, NSP2, NSP3, NSP4; p-IKK with NSP2, NSP3, NSP6, and p-NF $\kappa$ B with NSP2. Similarly, through confocal microscopy it was observed that PPAR $\gamma$  colocalizes with NSP1 and NSP3, RXR with NSP1, p-IKK with NSP2, and p-NF $\kappa$ B with NSP5. Since analysis with recombinant protein, NSP1 and NSP3 bind to PPAR $\gamma$ , and bind and co-localized in MA104, it is probable that they are the proteins responsible for inhibiting this inflammatory transcription factor. It has been reported that rotavirus NSP1 inhibits NF $\kappa$ B activation 5 to 7 h.p.i (Graff *et al.*, 2009). In our work, the time evaluated was at 12 h.p.i. for RRV and /or 36 h.p.t., where it was observed that the cellular infection was asynchronous. For this reason, we acknowledge that other transient bindings may occur between the different NSPs and the proteins of the cell. This can be presented for the MOI (0.8) used and because the amount of virus that enters the cells is

not homogeneously even, affecting the number and size of the viroplasm, which is dependent on the number of particles that enter the cells (Carreño-Torres *et al.*, 2010).

#### *The RRV infection affects the expression of cytoplasmic and nuclear PPAR $\gamma$*

The study aimed to find if the expression level of cytoplasmic or nuclear PPAR $\gamma$  protein is affected by RRV infection. The expression of PPAR $\gamma$  and NF $\kappa$ B proteins was analyzed in isolated nuclei and cytoplasm of RRV infected cells (MOI 0.8) 12 h.p.i., and treated with 153 mM TZD, 10  $\mu$ M GW9662 or 100  $\mu$ M CUR for 12 h. Similarly, non-infected cells transfected with NSPs and treated with TZD or CUR, were evaluated. When evaluating the PPAR $\gamma$  protein, through the ELISA, in non-infected cells, the absorbance was 0.145 $\pm$ 0.009, and in RRV infected cells 0.219 $\pm$ 0.063 (\*\*p: 0.0071) (Fig. 5a). The nuclei were

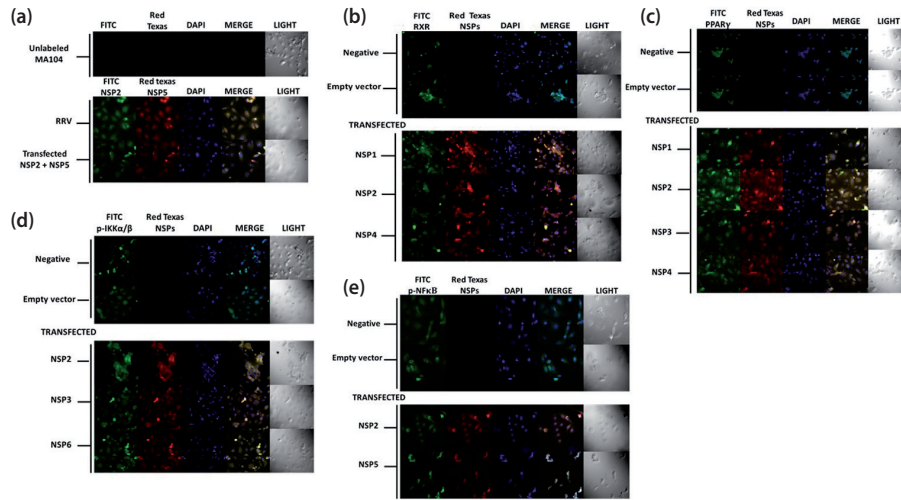


Fig. 4

**Confocal microscopy**

(a-f) Representative images of the focal plane Z with 2  $\mu$ m of thickness, detection of the colocalization of the RXR, PPAR $\gamma$ , p-IKK $\alpha/\beta$ , p-NF $\kappa$ B and viral NSPs proteins.

**Table 4. Co-localization between rotavirus nonstructural proteins and proteins related to PPAR $\gamma$ -NF $\kappa$ B pathway**

Sample	Pearson's coefficient	Overlap coefficient	Manders' coefficients	
Unlabeled MA104	0.178	0.179	M1=0.592	M2=0.207
<b>Positive control</b>				
RRV	0.499	0.546	M1=0.927	M2=0.968
NSP2+NSP5	0.43	0.572	M1=0.998	M2=0.86
<b>RXR</b>				
Negative control	0.264	0.268	M1=0.118	M2=0.987
Empty vector (Hygro)	0.077	0.078	M1=0.014	M2=0.969
NSP1	0.436	0.549	M1=0.997	M2=0.914
<b>PPAR<math>\gamma</math></b>				
Negative control	0.064	0.065	M1=0.0070	M2=1.0
Empty vector (Hygro)	0.067	0.066	M1=0.0070	M2=0.993
NSP1	0.505	0.542	M1=0.903	M2=0.918
NSP3	0.519	0.545	M1=0.811	M2=0.942
<b>p-IKK<math>\alpha/\beta</math></b>				
Negative control	0.016	0.017	M1=0.0	M2=0.92
Empty vector (Hygro)	0.0040	0.0090	M1=0.0	M2=0.901
NSP2	0.548	0.614	M1=0.995	M2=0.923
<b>p-NF<math>\kappa</math>B</b>				
Negative control	0.023	0.026	M1=0.0010	M2=0.794
Empty vector (Hygro)	0.017	0.018	M1=0.0010	M2=0.633
NSP5	0.715	0.725	M1=0.939	M2=0.984

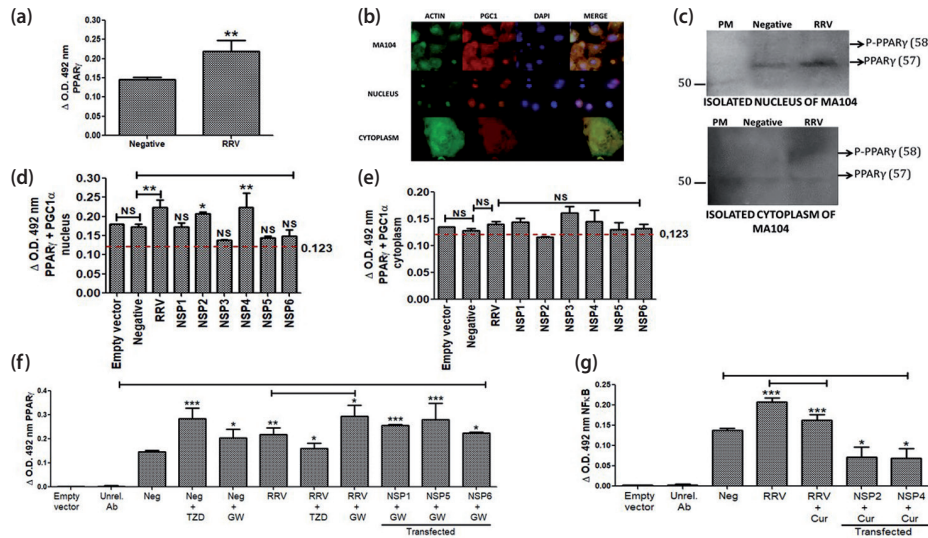


Fig. 5

#### The RRV infection affects the expression of cytoplasmic and nuclear PPAR $\gamma$

Capture ELISA of the expression of PPAR $\gamma$  protein in MA104 rotavirus infected cells (a). Epi-immunofluorescence of PGC1 and actin expression in cytoplasm and nucleus (b). Western blot of the expression of PPAR $\gamma$  and p-PPAR $\gamma$  proteins in nucleus and cytoplasm (c). Capture ELISA of PPAR $\gamma$ -PGC1 proteins in nucleus and cytoplasm of MA104 cells transfected with plasmids expressing NSPs of RRV (d-e). Capture ELISA of the expression of PPAR $\gamma$  and NF $\kappa$ B proteins in MA104 cells transfected with plasmids expressing NSPs of RRV and treated with thiazoglitazone, curcumin or GW9662 inhibitor (f-g).

isolated and representative images of the epifluorescence using specific anti-actin and anti-PGC1 $\alpha$  antibodies were taken (Fig. 5b). Two bands in the cytoplasmic fraction and the nuclear fraction were detected through the Western blot, which corresponded to PPAR $\gamma$  and p-PPAR $\gamma$ . In the cytoplasmic fraction, the band correspondent to p-PPAR $\gamma$  is 28% more intense in comparison with the PPAR $\gamma$  band in uninfected and infected cells. In the nuclear fraction, the band correspondent to PPAR $\gamma$ , in infected cells, is 74% more intense in comparison with the band in non-infected cells; the band correspondent to p-PPAR $\gamma$  is not observed in this fraction (Fig. 5c). When evaluating the binding between proteins, through the ELISA, in the cytoplasmic fraction, there were no differences in the expression between PPAR $\gamma$  and PGC1 $\alpha$  proteins, in non-infected cells, infected, or transfected cells. At the nuclear level, the binding between PPAR $\gamma$  and PGC1 $\alpha$  in infected cells was  $0.224 \pm 0.028$ , and in cells transfected with plasmids was, for NSP2,  $0.207 \pm 0.006$ , and NSP4,  $0.224 \pm 0.052$  (Fig. 5d-e). In non-infected, nor transfected cells, the PPAR $\gamma$  absorbance was  $0.145 \pm 0.009$ , while the expression of this protein increases in non-infected cells treated with TZD at  $0.284 \pm 0.062$ ; in non-infected cells treated with the GW9662 inhibitor, the absorbance increased to  $0.204 \pm 0.052$  in comparison with non-infected cells. When the cells are infected with rotavirus, the protein expression increases to  $0.218 \pm 0.049$  in comparison with non-infected cells. When treating infected cells with

TZD, the protein expression decreases to  $0.159 \pm 0.033$  in comparison with the infected cells. When treating the infected cells with the GW9662 inhibitor, the protein expression increases to  $0.293 \pm 0.065$  in comparison with the infected cells. When transfecting the cells with each of the plasmids expressed for each of the NSPs and treating them with TZD, no changes were observed in the PPAR $\gamma$  expression in non-infected, nor treated cells. When the cells were transfected with each of the plasmids that express NSPs and treated with the GW9662 inhibitor, the expression of PPAR $\gamma$  in the cells transfected with NSP1 increased to  $0.256 \pm 0.007$ , NSP5 to  $0.279 \pm 0.098$ , and NSP6 to  $0.224 \pm 0.005$  in comparison with the non-infected, nor transfected cells (Fig. 5f). In the non-infected nor transfected cells, the absorbance of NF $\kappa$ B was  $0.110 \pm 0.025$ . The NF $\kappa$ B expression in non-infected cells treated with CUR increased to  $0.141 \pm 0.008$  in comparison with the non-infected nor treated cells. In infected cells, the NF $\kappa$ B expression increased to  $0.193 \pm 0.068$  in comparison with the non-infected cells. When treating infected cells with CUR, the NF $\kappa$ B expression decreased to  $0.162 \pm 0.019$ , in comparison with untreated infected cells. When the cells were transfected with each of the plasmids that express each NSP and treated with curcumin, it was observed that NF $\kappa$ B in the cells transfected with NSP2 decreases to  $0.131 \pm 0.013$ , and, with NSP4, to  $0.075 \pm 0.004$  in comparison with non-infected, nor transfected cells (Fig. 5g). This result suggests that RRV infection activates mechanisms

that phosphorylate PPAR $\gamma$  leading to its inactivation. The above, may be due to the role of PPAR $\gamma$  being regulated by post-translational modifications like phosphorylation, SUMOylation, and ubiquitination. When PPAR $\gamma$  is modified by acetylation, it induces the PPAR $\gamma$  function in the absence of an external ligand; suggesting that the acetylation of PPAR $\gamma$  is an activation mechanism of PPAR $\gamma$  independent of the ligand (Jiang *et al.*, 2014). The phosphorylation is the most important post-translational modification that affects PPAR $\gamma$  activity. The PPAR $\gamma$  phosphorylation by MAPK results in the inhibition of protein transactivation both dependent and independent of the ligand, and inhibits PPAR $\gamma$  activity (Sozio *et al.*, 2011). We also observed that the PPAR $\gamma$  expression increased significantly when the non-infected cells were treated with a thiazolidinedione or GW9662 inhibitor, an irreversible and selective PPAR $\gamma$  antagonist (Seargent and Yates, 2004). Similarly, when the cells are infected with RRV, they increase the PPAR $\gamma$  expression significantly. These results suggest that thiazolidinedione inhibits the phosphorylation of PPAR $\gamma$ , altering the PPAR $\gamma$  levels directly or indirectly. It has been reported that cyclin-dependent kinase 5 (Cdk5) phosphorylates the nuclear receptor PPAR $\gamma$ . This PPAR $\gamma$  modification does not alter its adipogenic capacity but leads to the deregulation of many genes whose expression is altered. The phosphorylation of PPAR $\gamma$  by Cdk5 is blocked by anti-diabetic PPAR $\gamma$  ligands, such as rosiglitazone and MRL24 (Choi *et al.*, 2010). In our work, we found that in infected cells or cells transfected with NSP1, NSP5, and NSP6, treated with GW9662, the PPAR $\gamma$  expression increases. The same result was reported when infecting with rotavirus, finding an increase in cellular proteins PPAR $\gamma$ , NF $\kappa$ B, PDI, Hsc70, COX-2, and ROS (Gómez *et al.*, 2016), which were reduced when treating the infected cells with pioglitazone, reducing the number of generated viruses simultaneously. It was hypothesized that rotavirus infection induces a pro-inflammatory response in the host cells, benefiting the infection process, and that the interference in the inflammatory pathways involved leads to a decrease of the infectious elements (Guerrero and Acosta, 2016; Gómez *et al.*, 2016). It has been observed that the treatment with rosiglitazone provokes a significant decrease in the HIV-1 viral infection in macrophages (Potula *et al.*, 2008). It has also been found to reduce the influenza viral load and decrease the production of cytokines and chemokines in mice infected with influenza and treated with rosiglitazone compared with the controls (Gopal *et al.*, 2019). The PPAR $\gamma$  agonists have beneficial effects in the inflammatory response suppression during the infection by the respiratory syncytial virus (RSV) (Arnold *et al.*, 2007).

In this work, RRV infected cells or cells transfected with NSP2, and NSP4 increased the NF $\kappa$ B expression sig-

nificantly and when treated with CUR, decreased the NF $\kappa$ B expression and RRV infection significantly, supporting the idea that the rotavirus induces a pro-inflammatory response, benefiting the infectious process and its interference reduces the infection. It has been known that curcumin inhibits the NF $\kappa$ B pathway expression and downregulates the pro-inflammatory cytokines such as interleukin (IL)-1, IL-6, IL -8, and tumor necrosis factor (TNF- $\alpha$ ) (Liu *et al.*, 2007; Kim *et al.*, 2012). NF $\kappa$ B inhibitor drugs like caffeic acid phenethyl ester (CAPE), resveratrol Bay11-7082, and parthenolide inhibit the NF $\kappa$ B activation and reduce the SARS-CoV inflammation in mice (DeDiego *et al.*, 2014). The PPAR $\gamma$  activation represents an efficient therapeutic strategy to counteract a cytokine storm. The synthetic PPAR $\gamma$  agonists have anti-inflammatory properties that make them promising candidates to treat inflammation in severe viral diseases (Ciavarella *et al.*, 2020; Abdelrahman *et al.*, 2005; Belvisi *et al.*, 2006).

From this work, it can be concluded that during the RRV infection, RXR binds to NSP1, PPAR $\gamma$  binds to NSP1 and NSP3, p-IKK $\alpha$ / $\beta$  binds to NSP2, NF $\kappa$ B binds to NSP5. Phosphorylated PPAR $\gamma$  is present in the cytoplasm, and the PPRE transcriptional activity is diminished. Overall, it suggests that RRV activates the inflammatory pathway, increasing the NF $\kappa$ B expression and possibly inactivating PPAR $\gamma$  when PPAR $\gamma$  is phosphorylated in the cytoplasm inhibiting its translocation to the nucleus.

**Supplementary information** is available in the online version of paper.

## References

- Abdelrahman M, Sivarajah A, Thiemermann C (2005): Beneficial effects of PPAR-gamma ligands in ischemia-reperfusion injury, inflammation and shock. *Cardiovasc. Res.* 65 (4), 772-781. <https://doi.org/10.1016/j.cardiores.2004.12.008>
- Acta 14-2017 de 2017: Comité de Ética, Universidad Nacional de Colombia.
- Arias CE, Silva D, López S (2015): Rotavirus entry: a deep journey into the cell with several exits. *J. Virol.* 9 (2), 890-893. <https://doi.org/10.1128/JVI.01787-14>
- Arnold R, Neumann M, König W (2007): Peroxisome proliferator-activated receptor-gamma agonists inhibit respiratory syncytial virus-induced expression of intercellular adhesion molecule-1 in human lung epithelial cell. *Immunology.* 121 (1), 71-81. <https://doi.org/10.1111/j.1365-2567.2006.02539.x>
- Barro M, Patton JT (2005): Rotavirus nonstructural protein 1 subverts innate immune response by inducing degradation of IFN regulatory factor 3. *PNAS.* 102 (11), 4114-4119. <https://doi.org/10.1073/pnas.0408376102>

- Belvisi MG, Hele DJ, Birrell MA (2006): Peroxisome proliferator-activated receptor gamma agonists as therapy for chronic airway inflammation. *Eur. J. Pharmacol.* 533 (1-3), 101-109. <https://doi.org/10.1016/j.ejphar.2005.12.048>
- Bolte S, Cordelières FP (2006): A guided tour into subcellular colocalization analysis in light microscopy. *J. Micro.* 224(3), 213-232. <https://doi.org/10.1111/j.1365-2818.2006.01706.x>
- Bhowmick R, Halder UC, Chattopadhyay S et al. (2012): Rotaviral Enterotoxin Nonstructural Protein 4 Targets Mitochondria for Activation of Apoptosis during Infection. *J. Biol. Chem.* 287 (42), 35004-35020. <https://doi.org/10.1074/jbc.M112.369595>
- Camini FC, da Silva Caetano CC, Almeida LT, de Brito Magalhães CL (2017): Implications of oxidative stress on viral pathogenesis. *Arch. Virol.* 162, 907-917. <https://doi.org/10.1007/s00705-016-3187-y>
- Carreño-Torres JJ, Gutiérrez M, Arias CF, López S, Isa P (2010): Characterization of viroplasm formation during the early stages of rotavirus infection. *Virol. J.* 29 (7), 350. <https://doi.org/10.1186/1743-422X-7-350>
- Choi JH, Banks AS, Estall JL et al. (2010): Anti-diabetic drugs inhibit obesity-linked phosphorylation of PPAR gamma by Cdk5. *Nature.* 466 (7305), 451-456. <https://doi.org/10.1038/nature09291>
- Ciavarella C, Motta I, Valente S, Pasquinelli G (2020): Pharmacological (or synthetic) and nutritional agonists of PPAR- $\gamma$  as candidates for cytokine storm modulation in COVID-19 disease. *Molecules.* 25 (9), 2076. <https://doi.org/10.3390/molecules25092076>
- Clark, R (2002): The role of PPARs in inflammation and immunity. *J. Leuk. Biol.* 71 (3), 388-400.
- Crawford SE, Ramani S, Tate JE et al. (2017): Rotavirus infection. *Nat. Rev. Dis. Primers.* 3, 17083-17122. <https://doi.org/10.1038/nrdp.2017.83>
- DeDiego ML, Nieto-Torres JL, Regla-Nava JA, Jimenez-Guardeño JM, Fernandez-Delgado R, Fett C, Castaño-Rodríguez C, Perlman S, Enjuanes L (2014): Inhibition of NF- $\kappa$ B-mediated inflammation in severe acute respiratory syndrome coronavirus-infected mice increases survival. *J. Virol.* 88 (2), 913-924. <https://doi.org/10.1128/JVI.02576-13>
- Deng L, Zeng Q, Wang M et al. (2018): Suppression of NF- $\kappa$ B activity: A viral immune evasion mechanism. *Viruses.* 10 (8), 409. <https://doi.org/10.3390/v10080409>
- Deo RC, Groft CM, Rajashankar KR, Burley SK (2002): Recognition of the rotavirus mRNA 3' consensus by an asymmetric NSP3 homodimer. *Cell.* 108, 71-81. [https://doi.org/10.1016/S0092-8674\(01\)00632-8](https://doi.org/10.1016/S0092-8674(01)00632-8)
- Echeverri NP, Mockus I (2010): Cellular mechanisms in response to stress: sirtuin. *Revista de la facultad de medicina.* 58 (3), 221-232.
- Estes MK, Cohen J (1989): Rotavirus gene structure and function. *Microbiol. Rev.* 53 (4), 410. <https://doi.org/10.1128/mr.53.4.410-449.1989>
- Feng N, Sen A, Nguyen H, Hoshino Y, Deal EM, Greenberg HB (2009): Variation in antagonism of the interferon response to rotavirus NSP1 results in differential infectivity in mouse embryonic fibroblasts. *J. Virol.* 83, 6987-6994. <https://doi.org/10.1128/JVI.00585-09>
- Firth AE, Brierley I (2012): Non-canonical translation in RNA viruses. *J. Gen. Virol.* 93, 1385-1409. <https://doi.org/10.1099/vir.0.042499-0>
- Fuchs E, Flügge G (2004): Cellular consequences of stress and depression. *Dial. In Clin. Neurosci.* 6 (2), 171-183. <https://doi.org/10.31887/DCNS.2004.6.2/efuchs>
- Genolet R, Wahli W, Michalik L (2004): PPARs as drug targets to modulate inflammatory responses? *Curr. Drug Targets Inflamm. Allergy* 4, 361-375. <https://doi.org/10.2174/1568010042634578>
- Gómez D, Muñoz N, Guerrero R, Acosta O, Guerrero CA (2016): PPAR $\gamma$  agonists as an anti-inflammatory treatment inhibiting rotavirus infection of small intestinal villi. *PPAR research.* 2016, 4049373. <https://doi.org/10.1155/2016/4049373>
- Gopal R, Mendy A, Marinelli MA et al. (2019): Peroxisome proliferator-activated receptor gamma (PPAR $\gamma$ ) suppresses inflammation and bacterial clearance during influenza-bacterial super-infection. *Viruses.* 11 (6), 505. <https://doi.org/10.3390/v11060505>
- Graff JW, Ettayebi K, Hardy ME (2009): Rotavirus NSP1 inhibits NF $\kappa$ B activation by inducing proteasome-dependent degradation of  $\beta$ -TrCP: a novel mechanism of IFN antagonism. *PLoS Pathog.* 5, e1000280. <https://doi.org/10.1371/journal.ppat.1000280>
- Guerrero CA, Pardo P, Rodríguez V, Guerrero R, Acosta O (2013): Inhibition of rotavirus ECwt infection in ICR suckling mice by N-acetylcysteine, peroxisome proliferator-activated receptor gamma agonists and cyclooxygenase-2 inhibitors. *Memórias do Instituto Oswaldo Cruz.* 108 (6), 741-754. <https://doi.org/10.1590/0074-0276108062013011>
- Guerrero CA, Acosta O (2016): Inflammatory and oxidative stress in rotavirus infection. *World J. Virol.* 5 (2), 38-62. <https://doi.org/10.5501/wjv.v5.i2.38>
- Guerrero CA, Murillo A, Acosta O (2012): Inhibition of rotavirus infection in cultured cells by N-acetyl-cysteine, PPAR $\gamma$  agonists and NSAIDs. *Antivir. Res.* 96 (1), 1-12. <https://doi.org/10.1016/j.antiviral.2012.06.011>
- Guerrero CA, Moreno LP (2012): Rotavirus receptor proteins Hsc70 and integrin  $\alpha\beta$ 3 are located in the lipid microdomains of animal intestinal cells. *Acta Virol.* 56, 63-70. [https://doi.org/10.4149/av\\_2012\\_01\\_63](https://doi.org/10.4149/av_2012_01_63)
- Guerrero CA, Méndez E, Zárate S, Isa P, López S, Arias CF (2000): Integrin  $\alpha\beta$ 3 mediates rotavirus cell entry. *PNAS.* 97 (26), 14644-14649. <https://doi.org/10.1073/pnas.250299897>
- Gutiérrez M, Isa P, Sánchez C, Pérez J, Espinosa R, Arias CF, López S (2010): Different rotavirus strains enter MA104 cells through different endocytic pathways: the role of clathrin-mediated endocytosis. *J. Virol.* 84 (18), 9161-9169. <https://doi.org/10.1128/JVI.00731-10>
- Hsieh WC, Lan BS, Chen YL, Yao C, Chuang HC, Su IJ (2010): Efficacy of peroxisome proliferator activated receptor agonist in the treatment of virus-associated hae-

- mophagocytic syndrome in a rabbit model. *Antivir. Ther.* 15 (1), 71–81. <https://doi.org/10.3851/IMPI490>
- Huang J, Hume AJ, Abo KM *et al.* (2020): SARS-CoV-2 Infection of pluripotent stem cell-derived human lung alveolar type 2 cells elicits a rapid epithelial-intrinsic inflammatory response. *Cell Stem Cell*. bioRxiv (Preprint). <https://doi.org/10.1101/2020.06.30.175695>
- Huang S, Zhu B, Cheon IS *et al.* (2019): PPAR- $\gamma$  in macrophages limits pulmonary inflammation and promotes host recovery following respiratory viral infection. *J. Virol.* 93 (9), e00030–19. <https://doi.org/10.1128/JVI.00030-19>
- Isa P, Arias CF, López S (2006): Role of sialic acids in rotavirus infection. *Glycoconj. J.* 23 (1–2), 27–37. <https://doi.org/10.1007/s10719-006-5435-y>
- Ivanov AV, Bartosch B, Isaguliantz M (2017): Oxidative Stress in Infection and Consequent Disease. *Oxidative Med. Cell. Long.* 2017,3. <https://doi.org/10.1155/2017/3496043>
- Jarrar MH, Baranova A (2007): PPAR $\gamma$  activation by thiazolidinediones (TZDs) may modulate breast carcinoma outcome: the importance of interplay with TGF $\beta$  signalling. *J. Cell. Mol. Med.* 11 (1), 71–87. <https://doi.org/10.1111/j.1582-4934.2007.00003.x>
- Jiang X, Ye X, Guo W, Lu H, Gao Z (2014): Inhibition of HDAC3 promotes ligand-independent PPAR $\gamma$  activation by protein acetylation. *J. Mol. Endocrinol.* 53 (2), 191–200. <https://doi.org/10.1530/JME-14-0066>
- Kapadia R, Yi JH, Vemuganti R (2008): Mechanisms of anti-inflammatory and neuroprotective actions of PPAR-gamma agonists. *Frontiers in Bioscience: a journal and virtual library.* 13, 1813–1826. <https://doi.org/10.2741/2802>
- Kim JH, Gupta SC, Park B, Yadav VR, Aggarwal BB (2012): Turmeric (*Curcuma longa*) inhibits inflammatory nuclear factor (NF)- $\kappa$ B and NF- $\kappa$ B-regulated gene products and induces death receptors leading to suppressed proliferation, induced chemosensitization, and suppressed osteoclastogenesis. *Mol. Nutrition Food Res.* 56 (3), 454–465. <https://doi.org/10.1002/mnfr.201100270>
- Kumar N, Xin Z, Liang Y, Ly H, Liang Y (2008): NF- $\kappa$ B signaling differentially regulates influenza virus RNA synthesis. *J. Virol.* 82 (20), 9880–9889. <https://doi.org/10.1128/JVI.00909-08>
- Lauxmann MA, Santucci NE, Aufrán-Gómez AM (2020): The SARS-CoV-2 coronavirus and the COVID-19 outbreak. *Int. Braz. J. Urol.* 46 (Suppl. 1), 6–18. <https://doi.org/10.1590/s1677-5538.ibju.2020.s101>
- Lawrence, T (2009): The nuclear factor NF-kappaB pathway in inflammation. *Cold Spring Harbor Perspect. Biol.* 1 (6), a001651. <https://doi.org/10.1101/cshperspect.a001651>
- Li G, Fan Y, Lai Y *et al.* (2020): Coronavirus infections and immune responses. *J. Med. Virol.* 92 (4), 424–432. <https://doi.org/10.1002/jmv.25685>
- Liu T, Zhang L, Joo D, Sun SC (2007): NF- $\kappa$ B signaling in inflammation. *Sign. Transd. Target. Ther.* 2, 17023. <https://doi.org/10.1038/sigtrans.2017.23>
- Londrigan SL, Hewish MJ, Thomson MJ, Sanders GM, Mustafa H, Coulson BS (2000): Growth of rotaviruses in continuous human and monkey cell lines that vary in their expression of integrins. *J. Gen. Virol.* 81, 2203–2213. <https://doi.org/10.1099/0022-1317-81-9-2203>
- Martin, H (2010): Role of PPAR-gamma in inflammation. Prospects for therapeutic intervention by food components. *Mut. Res.* 690 (1–2), 57–63. <https://doi.org/10.1016/j.mrfmmm.2009.09.009>
- Moreno LY, Guerrero CA, Acosta O (2016): Protein disulfide isomerase and heat shock cognate protein 70 interactions with rotavirus structural proteins using their purified recombinant versions. *Revista Colombiana de Biotecnología.* 18 (1), 33–48. <https://doi.org/10.15446/rev.colomb.biote.v18n1.57714>
- Moreno LY, Guerrero CA, Acosta O (2013): Expression and purification of rotavirus structural proteins VP5\* and VP8\* in bacteria *E. coli* BL21(DE3). *Rev. Colomb. Biotecnol.* 15 (1), 82–97.
- Pesavento J, Crawford SE, Estes MK, Venkataram Prasad BV (2006): Rotavirus proteins: structure and assembly. *CTMI.* 309, 189–219. [https://doi.org/10.1007/3-540-30773-7\\_7](https://doi.org/10.1007/3-540-30773-7_7)
- Piron M, Vende P, Cohen J, Poncet D (1998): Rotavirus RNA-binding protein NSP3 interacts with eIF4GI and evicts the poly(A) binding protein from eIF4F. *EMBO J.* 17 (19), 5811–5821. <https://doi.org/10.1093/emboj/17.19.5811>
- Potula R, Ramirez SH, Knipe B *et al.* (2008): Peroxisome proliferator-activated receptor-gamma activation suppresses HIV-1 replication in an animal model of encephalitis. *AIDS (London, England).* 22 (13), 1539–1549. <https://doi.org/10.1097/QAD.0b013e3283081e08>
- Prieto I, Hervas-Stubbs S, Garcia-Granero M, Berasain C, Riezu-Boj JJ, Lasarte JJ, Sarobe P, Prieto J, Borrás-Cuesta F (1995): Simple strategy to induce antibodies of distinct specificity: application to the mapping of gp120 and inhibition of HIV-1 infectivity. *Eur. J. Immunol.* 25, 877–883. <https://doi.org/10.1002/eji.1830250403>
- Rainsford EW, Malcolm MA (2007): Characterization of the NSP6 protein product of rotavirus gene 11. *Virus Res.* 130 (1–2), 193–220. <https://doi.org/10.1016/j.virusres.2007.06.011>
- Rauwel B, Mariamé B, Martin H *et al.* (2010): Activation of peroxisome proliferator-activated receptor gamma by human cytomegalovirus for de novo replication impairs migration and invasiveness of cytotrophoblasts from early placentas. *J. Virol.* 84 (6), 2946–2954. <https://doi.org/10.1128/JVI.01779-09>
- Rico J, Perez C, Guerrero R, Hernandez J, Guerrero C, Acosta O (2020): Implication of heat shock proteins in rotavirus entry into Reh cells. *Acta Virol.* 64 (4), 433–450. [https://doi.org/10.4149/av\\_2020\\_406](https://doi.org/10.4149/av_2020_406)
- Rivera M, Guerrero CA, Acosta O (2020): Thiol/disulfide exchange occurs in rotavirus structural proteins during contact with intestinal villus cell surface. *Acta Virol.* 64 (1), 44–58. [https://doi.org/10.4149/av\\_2020\\_106](https://doi.org/10.4149/av_2020_106)
- Schindelin J, Arganda-Carreras I, Frise E, Kaynig V *et al.* (2012): Fiji: an open-source platform for biological-image analysis. *Nat. Methods.* 9 (7), 676–682. <https://doi.org/10.1038/nmeth.2019>

- Schwarz, KB (1996): Oxidative stress during viral infection: a review. *Free Radic. Biol. Med.* 21 (5), 41-649. [https://doi.org/10.1016/0891-5849\(96\)00131-1](https://doi.org/10.1016/0891-5849(96)00131-1)
- Seargent JM, Yates EA (2004): GW9662, a potent antagonist of PPAR gamma, inhibits growth of breast tumor cells and promotes the anticancer effects of the PPAR gamma agonist rosiglitazone, independently of PPAR gamma activation. *Br. J. Pharmacol.* 143 (8), 933-937. <https://doi.org/10.1038/sj.bjp.0705973>
- Sen A, Namsa ND, Feng N, Greenberg HB (2020): Rotavirus reprograms multiple interferon receptors and restricts their intestinal antiviral and inflammatory functions. *J. Virol.* 94 (6), e01775-e01819. <https://doi.org/10.1128/JVI.01775-19>
- Sen A, Feng N, Ettayebi K, Hardy ME, Greenberg HB (2009): IRF3 inhibition by rotavirus NSP1 is host cell and virus strain dependent but independent of NSP1 proteasomal degradation. *J. Virol.* 83, 10322-10335. <https://doi.org/10.1128/JVI.01186-09>
- Sozio MS, Yan Zeng CL, Liangpunsakul S, Crabb DW (2011): Activated AMPK inhibits PPAR- $\alpha$  and PPAR- $\gamma$  transcriptional activity in hepatoma cells. *Am. J. Physiol. Gastrointest. Liver Physiol.* 301, G739-G747. <https://doi.org/10.1152/ajpgi.00432.2010>
- Taylor RG, Walker DC, McInnes RR (1993): E. coli host strains significantly affect the quality of small scale plasmid DNA preparations used for sequencing. *Nucleic Acids Res.* 21, 1677-1678. <https://doi.org/10.1093/nar/21.7.1677>
- Trujillo Alonso V, Maruri Avidal L, Arias CF, López S (2011): Rotavirus Infection Induces the Unfolded Protein Response of the Cell and Controls It through the Non-structural Protein NSP3. *J. Virol.* 85 (23), 12594-12604. <https://doi.org/10.1128/JVI.05620-11>
- Villapol, S (2018): Roles of Peroxisome Proliferator-Activated Receptor Gamma on Brain and Peripheral Inflammation. *Cell. Mol. Neurobiol.* 38 (1), 21-132. <https://doi.org/10.1007/s10571-017-0554-5>
- Wang Z, Li Y, Yang X, Zhao J, Cheng Y, Wang J (2020): Mechanism and Complex Roles of HSC70 in Viral Infections. *Front. Microbiol.* 11, 1577. <https://doi.org/10.3389/fmicb.2020.01577>
- Yeligar SM, Ward JM, Harris FL, Brown LAS, Guidot DM, Cribbs SK (2017): Dysregulation of Alveolar Macrophage PPARgamma, NADPH Oxidases, and TGFbeta1 in Otherwise Healthy HIV-Infected Individuals. *AIDS Res. Hum. Retroviruses.* 33 (10), 1018-1026. <https://doi.org/10.1089/aid.2016.0030>
- Zárate S, Cuadras MA, Espinosa R, Romero P, Juárez KO, Camacho-Nuez M, Arias CF, López S (2003): Interaction of rotaviruses with Hsc70 during cell entry is mediated by VP5. *J. Virol.* 77, (13) 7254-7260. <https://doi.org/10.1128/JVI.77.13.7254-7260.2003>
- Zárate S, Espinosa R, Romero P, Guerrero CA, Arias CF, Lopez S (2000): Integrin alpha2beta1 mediates the cell attachment of the rotavirus neuraminidase-resistant variant nar3. *Virology.* 278, 50-54. <https://doi.org/10.1006/viro.2000.0660>
- Zhao J, He S, Minassian A, Li J, Feng P (2015): Recent advances on viral manipulation of NF- $\kappa$ B signaling pathway. *Curr. Opin. Virol.* 15, 103-111. <https://doi.org/10.1016/j.coviro.2015.08.013>
- Zulueta A, Colombo M, Peli V, Falleni M, Tosi D, Ricciardi M, Baisi A, Bulfamante G, Chiaramonte R, Caretti A (2018): Lung mesenchymal stem cells-derived extracellular vesicles attenuate the inflammatory profile of Cystic Fibrosis epithelial cells. *Cell Signal.* 51, 110-118. <https://doi.org/10.1016/j.cellsig.2018.07.015>